PERGAMON

International Journal of Solids and Structures 38 (2001) 5595–5604

INTERNATIONAL JOURNAL OF SOLIDS and STRUCTURES

www.elsevier.com/locate/ijsolstr

Theoretical models for void coalescence in porous ductile solids. II. Coalescence "in columns"

Mihai Gologanu [a], Jean-Baptiste Leblond [a,*], Josette Devaux [b]

[a] *Laboratoire de Modélisation en Mécanique, Université Pierre et Marie Curie, 8 rue du Capitaine Scott, 75015 Paris, France*
[b] *SYSTUS International, 84 boulevard Vivier-Merle, 69485 Lyon Cedex 03, France*

Received 3 May 2000

Abstract

As in the preceding paper, one studies coalescence of cavities in periodically voided ductile solids through consideration of a cylindrical representative volume element (RVE) containing a spheroidal void and subjected to some axisymmetric loading. However we now study the case where the major stress applied is no longer the axial one but the lateral one, so that the strain is mainly horizontal. This case has not been considered before in either FE micromechanical studies or theoretical models. It is envisaged here through both approaches. The basic idea of the model is that owing to the type of loading considered, the voids gradually concentrate along vertical columns. This is accounted for by schematizing the RVE as made of two coaxial cylinders, a highly porous, central one surrounded by a sound one. Just as in the case of coalescence in layers, the authors' recent extension of Gurson's model accounting for void shape is used to describe the behavior of the central zone whereas the sound one obeys von Mises' criterion. However, there is a major difference, namely that the sound outer region cannot become rigid here, since this would prohibit global flow. As a result, there is no more a sharp transition from pre-coalescence to coalescence but a gradual one. Comparison of the model predictions with the FE results exhibits a good agreement for a wide range of triaxialities.

Keywords: Ductile fracture; Void coalescence; Periodic medium; Void shape effects; Predictive model; Numerical simulations

1. Introduction

In all previous 2D (axisymmetric) FE micromechanical studies of void coalescence, and especially in the pioneering work of Koplik and Needleman, 1988, it was assumed that the major stress applied was the axial one ($\Sigma_{zz} > \Sigma_{xx} = \Sigma_{yy}$, where z denotes the direction of the axis of symmetry). As explained in Part I, this resulted in coalescence occurring within horizontal "layers". Also, previous theoretical models, such as those of Perrin, 1992, based on Rudnicki and Rice (1975) work on strain localization, Pardoen and

* Corresponding author. Tel.: +33-1-44-27-39-24; fax: +33-1-44-27-52-59.
E-mail address: leblond@lmm.jusien.fr (J.-B. Leblond).

0020-7683/01/$ - see front matter
PII: S0020-7683(00)00355-3

Hutchinson, 2000 and Benzerga, 2000, based on Thomason (1985) "coalescence criterion", only considered the case of a major axial stress.

We shall consider here the "opposite" case where the major stress applied is the lateral one ($\Sigma_{xx} = \Sigma_{yy} > \Sigma_{zz}$). It can be anticipated that in that case, due to lateral stretching and vertical shrinking, the intervoid distances will increase in the horizontal directions and decrease in the axial one, again resulting in a strain-induced anisotropy of the distribution of voids. However voids will now concentrate along vertical "columns" instead of horizontal "layers", so that coalescence will occur through necking of the vertical, and not horizontal, ligaments separating voids.

Coalescence "in columns" was very recently observed experimentally by Benzerga, 2000, although not in the situation envisaged here of a major lateral stress, but in laminated plates, for very prolate, aligned voids generated around elongated inclusions resulting from the rolling process. Also, Benzerga made the remark that although this type of coalescence is less detrimental than the other one (because formation of ruined columns has less severe consequences upon the stress bearing capacity of the material than that of ruined layers), it is of some importance in delamination of plates.

Following the same line of thought as for the modeling of coalescence in layers, one is naturally led to the idea of schematizing the RVE as made up of several zones, highly porous or sound. However, the porous region will now have to be a central cylinder surrounded by a sound one, instead of a porous layer lying between two sound ones. Again, the behavior of the sound central zone will be described by the Gologanu-LeblonA-Devaux (GLD) model (Gologanu, 1997; Gologanu et al., 1997), which is an extension of the well-known model of Gurson, 1977 accounting for void shape effects, while the surrounding sound one will naturally be assumed to obey von Mises' criterion and the associated flow rule.

However, there will be two main novelties with respect to the case of coalescence in layers. The first one, of rather technical nature, is that whereas the strain rate and stress fields will again be considered without harm as homogeneous in the porous central cylinder, such a hypothesis will become impossible in the surrounding sound cylinder. However this difficulty will be circumvented by some trick resorting to the (exact) model of Gurson, 1977 for *cylindrical* voids and avoiding the calculation of the entire mechanical fields within the sound zone. The second, more important difference is that it will no longer be possible for this zone to become rigid, because it is quite obvious that this would preclude any global flow of the RVE. Consequently, it will not be possible to clearly distinguish between a "pre-coalescence" phase and a "coalescence" one, the transition between the two being now a gradual, and not sudden, phenomenon.

It should be noted that precisely because of this, it seems an impossible task to extend previous models for coalescence in layers (Perrin, 1992; Pardoen and Hutchinson, 2000; Benzerga, 2000) to coalescence in columns. Indeed the theories they resort to (Rudnicki and Rice, 1975 condition of strain localization in Perrin's approach, Thomason, 1985 coalescence criterion in those of Pardoen and Hutchinson and Benzerga) are fundamentally based upon the assumption that the sound regions of the material become rigid when coalescence sets in. Therefore the approach proposed here, based on the mental division of the RVE into highly porous and sound zones, seems the only possible one for coalescence in columns.

Our model of coalescence in columns will be expounded first. The theoretical treatment will be somewhat more involved than for coalescence in layers, because of the non-uniformity of the strain rate and stress fields in the outer, sound cylinder. It will be given a compact format by using the notions of local and overall plastic dissipations, together with some parametrization of the GLD yield locus, applicable in particular to Gurson's yield locus for *cylindrical* voids. Comparisons with the results of some FE micromechanical simulations will be presented next. We shall only consider one initial porosity and an initially spherical void, but several triaxialities encompassing the range of practical interest. A good agreement between model predictions and numerical results will be evidenced in all cases.

2. Model for coalescence in columns

2.1. Generalities

As in Part I, we consider a cylindrical RVE containing a void the shape of which is assumed to initially be and subsequently approximately remain spheroidal. Again, the dimensions of the void are denoted a and b, and those of the cylinder, A and B (Fig. 1a). The RVE is subjected to some macroscopic axisymmetric ($\Sigma_{xx} = \Sigma_{yy}$) tensile ($\mathrm{tr}\,\Sigma > 0$) loading with predominant *lateral* stress ($\Sigma_{xx} > \Sigma_{zz}$). Its upper and lower surfaces are constrained to remain planar and the lateral one cylindrical; that is, the velocity $\mathbf{v}$ satisfies the following boundary conditions:

$$v_r = D_{xx} r \quad \text{for } r = B, \tag{1a}$$

$$v_z = D_{zz} z \quad \text{for } z = \pm A, \tag{1b}$$

where cylindrical coordinates are employed and D_{xx} ($= D_{yy}$) and D_{zz} denote the non-zero components of the macroscopic strain rate $\mathbf{D}$. The triaxiality

$$T \equiv \frac{\frac{1}{3}(2\Sigma_{xx} + \Sigma_{zz})}{\Sigma_{xx} - \Sigma_{zz}} \tag{2}$$

is assumed to be fixed during the whole mechanical history.

As already mentioned in Section 1, due to lateral stretching and axial contraction, the horizontal void spacing will increase and the vertical one decrease, resulting in a strain-induced anisotropy of the void distribution, so that coalescence of voids will occur through necking of the vertical intervoid ligaments (coalescence "in columns"). Following the same kind of idea as for coalescence in layers, we account for this strain-induced anisotropy by schematizing the RVE as made up of two coaxial cylinders (Fig. 1b). The central one, of radius D, is highly porous, while the surrounding one, of thickness $B - D$, is fully sound. The stress and strain rate fields are considered as homogeneous in the porous zone. The GLD model (Gologanu et al., 1997), accounting for void shape effects, is employed to describe its behavior; its equations were given in Section 2 of Part I. On the other hand, the mechanical fields within the surrounding sound cylinder, the behavior of which is obviously assumed to obey von Mises' criterion and the associated flow rule, are clearly inhomogeneous.

Our choice for the radius D of the central cylinder is again based on the consideration that since its behavior is to be described by the GLD model, it should logically be geometrically as close as possible to the RVE used for the derivation of that model, namely a spheroid confocal with the void. One thus obtains the new "confocality condition"

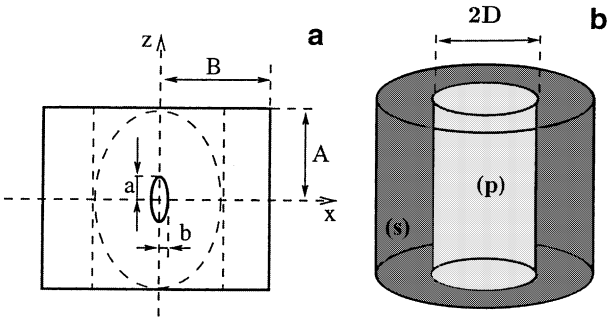

Fig. 1. The RVE considered in the model for coalescence in columns – (a) real RVE; (b) model composite structure.

$$D^2 - A^2 = b^2 - a^2 \Rightarrow D = \sqrt{A^2 + b^2 - a^2}. \tag{3}$$

Again, we denote by p the volume proportion of the central porous cylinder within the RVE and by $f^{(\mathrm{p})} \equiv 2ab^2/(3AD^2)$ the porosity in that zone; thus

$$p = \frac{D^2}{B^2}; \qquad f^{(\mathrm{p})} = \frac{f}{p}, \tag{4}$$

where $f \equiv 2ab^2/(3AB^2)$ denotes the porosity in the whole RVE. Again, more generally, we shall use upper indices (p) and (s) to denote quantities defined in the porous cylinder and the sound one whenever any confusion with some "macroscopic" quantity will be possible. For instance, we shall denote $\Sigma_{xx}^{(\mathrm{p})}$, $\Sigma_{zz}^{(\mathrm{p})}$ the (homogeneous) stresses in the porous zone, which differ from the overall stresses Σ_{xx}, Σ_{zz} in the whole RVE. On the other hand, the axial strain rate will simply be denoted D_{zz}, since the boundary condition (1b) obviously implies that $D_{zz}^{(\mathrm{p})} = D_{zz}^{(\mathrm{s})} \equiv D_{zz}$.

It has already been mentioned in Section 1, and is self-evident, that rigidity of the sound outer cylinder would prohibit any global flow of the RVE. Therefore, in contrast to the case of coalescence in layers, *the sound zone necessarily always remains plastic*. As a consequence, no clear distinction between a pre-coalescence period implying plasticity of the sound region and a coalescence one implying rigidity of this zone will be necessary; the transition between the two periods will no more be sudden but gradual, and they will be described by the same type of equations.

As a preliminary, let us derive the relation between the (homogeneous) strain rate $\mathbf{D}^{(\mathrm{p})}$ in the porous region and the macroscopic one, $\mathbf{D}$. It has already been mentioned that $D_{zz}^{(\mathrm{p})} = D_{zz}$. Also, since the sound zone is incompressible, $2D_{xx}^{(\mathrm{p})} + D_{zz}^{(\mathrm{p})} = (2D_{xx} + D_{zz})/p$. It follows that

$$\begin{cases} D_{xx}^{(\mathrm{p})} = D_{yy}^{(\mathrm{p})} = \frac{D_{xx}}{p} + \frac{1}{2}\left(\frac{1}{p} - 1\right)D_{zz} = \frac{1}{2p}\left(D_{xx} + D_{yy}\right) + \frac{1}{2}\left(\frac{1}{p} - 1\right)D_{zz}, \\ D_{zz}^{(\mathrm{p})} = D_{zz}, \end{cases} \tag{5}$$

which implies that

$$\begin{cases} \frac{\partial D_{xx}^{(\mathrm{p})}}{\partial D_{xx}} = \frac{\partial D_{yy}^{(\mathrm{p})}}{\partial D_{yy}} = \frac{\partial D_{xx}^{(\mathrm{p})}}{\partial D_{yy}} = \frac{\partial D_{yy}^{(\mathrm{p})}}{\partial D_{xx}} = \frac{1}{2p}, \\ \frac{\partial D_{xx}^{(\mathrm{p})}}{\partial D_{zz}} = \frac{\partial D_{yy}^{(\mathrm{p})}}{\partial D_{zz}} = \frac{1}{2}\left(\frac{1}{p} - 1\right), \\ \frac{\partial D_{zz}^{(\mathrm{p})}}{\partial D_{zz}} = 1. \end{cases} \tag{6}$$

2.2. Calculation of stresses

Because of axisymmetry and incompressibility of the sound outer cylinder, it is easy to determine the velocity field in this region, as a function of the components of the macroscopic strain rate. The calculation of the microscopic stresses in the outer cylinder and of the macroscopic stresses then follows from the equations expressing radial equilibrium, von Mises' criterion and the associated flow rule. This calculation is analogous to that performed by Gurson, 1977 to derive the overall criterion of a hollow cylinder, the sole difference being that here the inner boundary is no longer traction-free. However one can propose a shorter, though somewhat more abstract, approach based upon the notions of plastic microscopic (w) and macroscopic (W) dissipations. By these expressions, one means functions of the microscopic ($\mathbf{d}$) or macroscopic ($\mathbf{D}$) strain rates such that

$$\boldsymbol{\sigma} = \frac{\partial w}{\partial \mathbf{d}}(\mathbf{d}); \qquad \boldsymbol{\Sigma} = \frac{\partial W}{\partial \mathbf{D}}(\mathbf{D}). \tag{7}$$

It has been shown by Gurson, 1977 that

$$W(\mathbf{D}) = \frac{1}{\Omega}\int_{\Omega} w(\mathbf{d}(\mathbf{v}))\,\mathrm{d}\Omega,$$

where Ω denotes both the domain occupied by the RVE and its volume, and $\mathbf{v}$ (which depends on $\mathbf{D}$) the solution of the plasticity problem compatible with the boundary conditions (1a) and (1b). It follows that, with obvious notations,

$$W(\mathbf{D}) = pW^{(\mathrm{p})}\left(\mathbf{D}^{(\mathrm{p})}\right) + \frac{1}{\Omega}\int_{\Omega^{(\mathrm{s})}} w^{(\mathrm{s})}(\mathbf{d}(\mathbf{v}))\,\mathrm{d}\Omega.$$

Now the second term in the right-hand side here, which involves an integral over the *sole sound region* $\Omega^{(\mathrm{s})}$, represents the overall plastic dissipation of a sound hollow cylinder with an *empty core*. Indeed it was noted above that the solution $\mathbf{v}$ in the outer cylinder is uniquely determined as a function of $\mathbf{D}$ by Eqs. (1a) and (1b) and thus is the same irrespective of whether the inner one is porous or empty. We shall use an upper index $(\mathrm{s}+\mathrm{v})$ ("sound + void") to denote quantities relative to this "auxiliary" structure consisting of a sound outer cylinder with an empty core. With this notation, the preceding expression becomes

$$W(\mathbf{D}) = pW^{(\mathrm{p})}\left(\mathbf{D}^{(\mathrm{p})}\right) + W^{(\mathrm{s}+\mathrm{v})}(\mathbf{D})$$

so that

$$\begin{aligned}\boldsymbol{\Sigma} &= \frac{\partial W}{\partial \mathbf{D}}(\mathbf{D}) = p\frac{\partial W^{(\mathrm{p})}}{\partial \mathbf{D}^{(\mathrm{p})}}(\mathbf{D}^{(\mathrm{p})}) : \frac{\partial \mathbf{D}^{(\mathrm{p})}}{\partial \mathbf{D}} + \frac{\partial W^{(\mathrm{s}+\mathrm{v})}}{\partial \mathbf{D}}(\mathbf{D})\\ &= p\boldsymbol{\Sigma}^{(\mathrm{p})}\left(\mathbf{D}^{(\mathrm{p})}\right) : \frac{\partial \mathbf{D}^{(\mathrm{p})}}{\partial \mathbf{D}} + \boldsymbol{\Sigma}^{(\mathrm{s}+\mathrm{v})}(\mathbf{D}).\end{aligned}$$

Using the values of the non-zero components of the fourth order tensor $\partial\mathbf{D}^{(\mathrm{p})}/\partial\mathbf{D}$ given by Eq. (6), one deduces the following expressions of Σ_{xx} and Σ_{zz} from the preceding equation:

$$\begin{cases}\Sigma_{xx} = \Sigma_{xx}^{(\mathrm{p})} + \Sigma_{xx}^{(\mathrm{s}+\mathrm{v})},\\ \Sigma_{zz} = (1-p)\Sigma_{xx}^{(\mathrm{p})} + p\Sigma_{zz}^{(\mathrm{p})} + \Sigma_{zz}^{(\mathrm{s}+\mathrm{v})}.\end{cases} \tag{8}$$

We shall now use the parametrization (A.2)–(A.4) of the GLD yield locus expounded in Appendix A. We first apply it to the stresses in the porous zone, replacing Σ_{xx}, Σ_{zz}, ϵ, λ, $\mathscr{A}$, $\mathscr{B}$, f by $\Sigma_{xx}^{(\mathrm{p})}$, $\Sigma_{zz}^{(\mathrm{p})}$, $\epsilon^{(\mathrm{p})}$, [1] $\lambda^{(\mathrm{p})}$, $\mathscr{A}^{(\mathrm{p})}$, $\mathscr{B}^{(\mathrm{p})}$, $f^{(\mathrm{p})}$. (No similar upper index is used for the other quantities involved, because this is more economical and will not raise any ambiguity.) Since by Eq. (A.7), $\epsilon^{(\mathrm{p})}$ is also the opposite of the sign of $(1-2\alpha_2)D_{xx}^{(\mathrm{p})} - \alpha_2 D_{zz}$ which is positive (because in practice $D_{xx}^{(\mathrm{p})} > 0$ and $D_{zz} < 0$ for the type of loading considered here), $\epsilon^{(\mathrm{p})}$ is negative. Therefore the parametrization of the yield locus of the porous zone reads

$$\begin{cases}\frac{\Sigma_{xx}^{(\mathrm{p})}}{\sigma_0} = (1-2\alpha_2)\mathscr{A}^{(\mathrm{p})}\left(\lambda^{(\mathrm{p})}\right) + [1+(1-2\alpha_2)\eta]\mathscr{B}^{(\mathrm{p})}\left(\lambda^{(\mathrm{p})}\right),\\ \frac{\Sigma_{zz}^{(\mathrm{p})}}{\sigma_0} = -2\alpha_2\mathscr{A}^{(\mathrm{p})}\left(\lambda^{(\mathrm{p})}\right) + (1-2\alpha_2\eta)\mathscr{B}^{(\mathrm{p})}\left(\lambda^{(\mathrm{p})}\right),\end{cases} \tag{9}$$

where

$$\begin{cases}\mathscr{A}^{(\mathrm{p})}\left(\lambda^{(\mathrm{p})}\right) \equiv \frac{1}{\sqrt{C}}\left[\sqrt{\lambda^{(\mathrm{p})2} + (g+1)^2} - \sqrt{\lambda^{(\mathrm{p})2} + q^2(g+f^{(\mathrm{p})})^2}\right],\\ \mathscr{B}^{(\mathrm{p})}\left(\lambda^{(\mathrm{p})}\right) \equiv \frac{1}{\kappa}\left[\operatorname{arg\,sinh}\left(\frac{\lambda^{(\mathrm{p})}}{q(g+f^{(\mathrm{p})})}\right) - \operatorname{arg\,sinh}\left(\frac{\lambda^{(\mathrm{p})}}{g+1}\right)\right],\end{cases} \tag{10}$$

[1] Note that just like ϵ, $\epsilon^{(\mathrm{p})}$ denotes a sign, not a (plastic) strain!

$\lambda^{(p)}$ being an arbitrary parameter. It is recalled that the parameters α_2, η, C, g, q, κ here are given by Eqs. (2), (5)–(12) of Part I, f being replaced by $f^{(p)}$.

Let us now consider the "auxiliary" (sound + void) structure. For such a hollow cylinder (Gurson, 1977), criterion is exact (for axisymmetric loadings, as considered here). Furthermore, the GLD model reproduces this exact solution, the parameters α_2, η, C, g, q, κ taking then the values $1/2$, 0, 1, 0, 1, $\sqrt{3}$ (see Gologanu et al., 1997). Therefore the parametrization defined by Eqs. (A.2)–(A.4) of Appendix A is applicable with these substitutions, and provided that f is replaced by the volume proportion p of the central empty core. Since $\epsilon^{(s+v)} \equiv \operatorname{sgn} D_{zz}$ (Eq. (A.7) with $\alpha_2 = 1/2$) is negative in practice, the parametrization reads

$$\begin{cases} \frac{\Sigma_{xx}^{(s+v)}}{\sigma_0} = \mathscr{B}^{(s+v)}\left(\lambda^{(s+v)}\right), \\ \frac{\Sigma_{zz}^{(s+v)}}{\sigma_0} = -\mathscr{A}^{(s+v)}\left(\lambda^{(s+v)}\right) + \mathscr{B}^{(s+v)}\left(\lambda^{(s+v)}\right), \end{cases} \tag{11}$$

where

$$\begin{cases} \mathscr{A}^{(s+v)}\left(\lambda^{(s+v)}\right) \equiv \sqrt{\lambda^{(s+v)2}+1} - \sqrt{\lambda^{(s+v)2}+p^2}, \\ \mathscr{B}^{(s+v)}\left(\lambda^{(s+v)}\right) \equiv \frac{1}{\sqrt{3}}\left[\operatorname{arg\,sinh}\left(\frac{\lambda^{(s+v)}}{p}\right) - \operatorname{arg\,sinh}\lambda^{(s+v)}\right], \end{cases} \tag{12}$$

$\lambda^{(s+v)}$ being another arbitrary parameter.

In fact, the parameters $\lambda^{(p)}$ and $\lambda^{(s+v)}$ are not independent, because they are tied to the strain rates $\mathbf{D}^{(p)}$ and $\mathbf{D}$ through Eq. (A.6) of Appendix A, and $\mathbf{D}^{(p)}$ and $\mathbf{D}$ are themselves tied through Eq. (5). Thus

$$\frac{\operatorname{tr}\mathbf{D}^{(p)}}{2\left[(1-2\alpha_2)D_{xx}^{(p)} - \alpha_2 D_{zz}\right]} + \eta = \frac{\kappa}{\sqrt{C}}\lambda^{(p)}, \tag{13a}$$

$$-\frac{\operatorname{tr}\mathbf{D}}{D_{zz}} = \sqrt{3}\lambda^{(s+v)}. \tag{13b}$$

Using Eq. (5), one then easily shows that

$$\frac{\kappa}{\sqrt{C}}\lambda^{(p)} = \frac{\sqrt{3}\lambda^{(s+v)}}{p + \sqrt{3}(1-2\alpha_2)\lambda^{(s+v)}} + \eta. \tag{14}$$

Eqs. (8)–(12), (14) express the stresses in terms of a single free parameter, $\lambda^{(s+v)}$. The value of this parameter may be determined by enforcing condition (2), where T denotes the overall triaxiality imposed.

2.3. Evolution of the strain, the porosity and the void shape

Once the parameter $\lambda^{(s+v)}$ is known, Eq. (13b) provides the value of the ratio D_{xx}/D_{zz}, and therefore those of D_{xx} and D_{zz} up to some positive multiplicative constant. The values of $D_{xx}^{(p)}$ and $D_{zz}^{(p)}$ then follow from Eq. (5).

Once $\mathbf{D}$ is known, the porosity rate is given by the classical (unmodified) evolution equation for f (Eq. (14) of Part I). Also, the evolution of the void shape parameter S is given by Eq. (15) of Part I with the appropriate replacements, that is

$$\dot{S} = h\left(D_{zz} - D_{xx}^{(p)}\right) + \left(\frac{1-3\alpha_1}{f^{(p)}} + 3\alpha_2 - 1\right)\operatorname{tr}\mathbf{D}^{(p)}. \tag{15}$$

The parameter h here is given by Eqs. (16) and (17) and the second term of Eq. (19) of Part I, f being replaced by $f^{(p)}$ and $T \equiv \frac{1}{3}(2\Sigma_{xx} + \Sigma_{zz})/(\Sigma_{xx} - \Sigma_{zz})$ by $T^{(p)} \equiv \frac{1}{3}(2\Sigma_{xx}^{(p)} + \Sigma_{zz}^{(p)})/(\Sigma_{xx}^{(p)} - \Sigma_{zz}^{(p)})$.

The above equations allow for the step-by-step calculation of all quantities of interest as functions of some "control parameter", for instance the overall equivalent cumulated strain

$$E_{\mathrm{eq}} \equiv \int_0^t \left(\tfrac{2}{3}\mathbf{D}' : \mathbf{D}'\right)^{1/2}(\tau)\mathrm{d}\tau = \int_0^t \tfrac{2}{3}(D_{xx} - D_{zz})(\tau)\mathrm{d}\tau \tag{16}$$

where $\mathbf{D}'$ denotes the deviator of $\mathbf{D}$.

3. Comparison with some finite element simulations

Finite element micromechanical simulations analogous to those of Koplik and Needleman, 1988 and those presented in Part I, but with a predominant lateral stress ($\Sigma_{xx} > \Sigma_{zz}$), have been performed. Only one initial porosity, namely $f_0 = 0.0104$, and an initially spherical void were considered. Also, equal values were taken for the initial diameter and height of the RVE. Triaxialities of 1/3, 2/3, 1 and 2 were considered. Computations were performed using the SYSTUS FE code developed by SYSTUS International. The results of these simulations will now be compared to the model predictions.

A value of 1.1 for Tvergaard (1981) parameter q_0 for spherical cavities will be used in the model, unless otherwise stated. This value is smaller than those used in Part I for coalescence in layers ($q_0 = 1.47$ and 1.6 for $f_0 = 0.0104$ and 0.0002 respectively). However, it is compatible with the finding of Gologanu, 1997 that smaller q_0 values must be used for loadings with two equal major principal stresses and one minor one, as considered here, than for loadings with one major principal stress and two equal minor ones, as considered in Part I. In fact, the value adopted is the one that provides the best possible agreement between numerical and theoretical curves at the beginning of the mechanical history (prior to coalescence).

Fig. 2 presents the comparison of numerical results and model predictions for the normalized stress $\Sigma_{\mathrm{eq}}/\sigma_0$, the porosity and the opposite of the void shape parameter. Fig. 2a exhibits a remarkable agreement for the overall stress–overall strain curves. For triaxialities of 2/3, 1 and 2, both the FE results and the model predictions involve a slow decrease of the normalized stress prior to coalescence followed by a quicker (although much less marked than for coalescence in layers) one during coalescence, with a smooth transition between the two regimes. For a triaxiality of 1/3, the model does not predict any coalescence, again in agreement with the numerical results. Fig. 2b shows the evolution of the porosity. The initially slow, then gradually quicker increase of f is again correctly reproduced by the model for $T = 2/3$, 1 and 2. On the other hand, both the numerical results and the model involve void closure for $T = 1/3$ (which is obviously why coalescence does not occur in that case). The explanation is that the initially spherical void grows into oblate shapes since $\Sigma_{xx} > \Sigma_{zz}$, thus becoming more and more "sensitive" to the axial stress which is *negative* for this triaxiality, and thereby collapses. Finally, Fig. 2c and d exhibit a qualitatively satisfactory, though poorer than before, agreement for the evolution of the void shape parameter. The discrepancy is obviously due to the fact that the evolution equation (15), which was designed for the pre-coalescence period, does not quite capture the specific evolution of the void shape during coalescence.

Just as for coalescence in layers, we shall finally show that it is essential to introduce both the division of the RVE into highly porous and sound zones and void shape effects into the model in order to get satisfactory predictions. The mental division of the RVE may easily be suppressed by setting $D = B$ (instead of $\sqrt{A^2 + b^2 - a^2}$; see Fig. 1). In fact, this just means using the GLD model to describe the behavior of the *whole RVE* instead of the sole porous zone, thereby completely forgetting about coalescence. Fig. 3a and b compare the numerical results with the theoretical ones obtained in that way, for the normalized stress and the porosity. Two values of Tvergaard's parameter q_0, 1.1 and 1.4, are used in order to show that it then becomes impossible to reproduce both the beginning and the end of the numerical curves, whatever the value of q_0 chosen (except for a triaxiality of 1/3, for which no coalescence occurs).

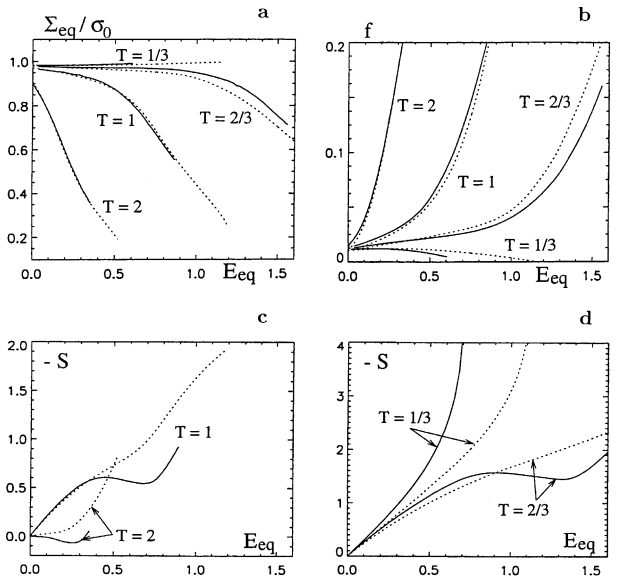

Fig. 2. Comparison of FE results (—) and model predictions (···) – (a) normalized stress; (b) porosity; (c) and (d) void shape parameter.

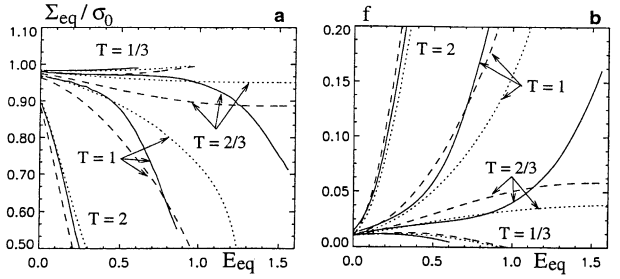

Fig. 3. Same as Fig. 2a and b, but for the simplified model considering only one, porous zone (GLD model) – (···): $q_0 = 1.1$; (- - -): $q_0 = 1.4$.

On the other hand, void shape effects may be suppressed in the model by using Gurson's original model (for spherical cavities), instead of the GLD model, to describe the behavior of the porous region. It is then logical to take $D = A$, in agreement with the second part of Eq. (3) with $a = b$. Fig. 4a and b show the results obtained in that way. The agreement of numerical and theoretical results is still good for $T = 1$ and 2, but the model now underestimates the ductility (overestimates the porosity) for $T = 2/3$. Also, it wrongly predicts void growth (and coalescence) instead of collapse for $T = 1/3$.

Appendix A. Parametrization of the GLD yield locus

The parametrization proposed emerges in a natural way from the derivation of the macroscopic yield criterion through homogenization (see e.g. Leblond and Perrin, 1996, for the simpler case of the Gurson model). It reads as follows:

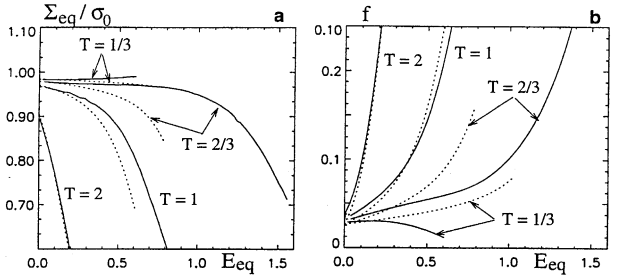

Fig. 4. Same as Fig. 2a and b, but for the simplified model using the Gurson model instead of the GLD model in the porous zone.

$$\begin{cases} \frac{\Sigma_{zz}-\Sigma_{xx}+\eta\Sigma_h}{\sigma_0} = \epsilon\mathscr{A}(\lambda), \\ \frac{\Sigma_h}{\sigma_0} = \mathscr{B}(\lambda), \end{cases} \tag{A.1}$$

where [2]

$$\epsilon \equiv \operatorname{sgn}(\Sigma_{zz} - \Sigma_{xx} + \eta\Sigma_h) \tag{A.2}$$

and

$$\begin{cases} \mathscr{A}(\lambda) \equiv \frac{1}{\sqrt{C}}\left[\sqrt{\lambda^2 + (g+1)^2} - \sqrt{\lambda^2 + q^2(g+f)^2}\right], \\ \mathscr{B}(\lambda) \equiv \frac{1}{\kappa}\left[\operatorname{arg\,sinh}\left(\frac{\lambda}{q(g+f)}\right) - \operatorname{arg\,sinh}\left(\frac{\lambda}{g+1}\right)\right], \end{cases} \tag{A.3}$$

λ being an arbitrary parameter. Indeed it is easy to check that if $\Sigma_{zz} - \Sigma_{xx} + \eta\Sigma_h$ and Σ_h are given by Eq. (A.1), then

$$\frac{C}{\sigma_0^2}(\Sigma_{zz} - \Sigma_{xx} + \eta\Sigma_h)^2 + 2q(g+1)(g+f)\cosh\left(\kappa\frac{\Sigma_h}{\sigma_0}\right) - (g+1)^2 - q^2(g+f)^2 = 0,$$

which is the analytical expression of the GLD yield criterion (see Eq. (3) of Part I).

Since

$$\Sigma_h \equiv 2\alpha_2\Sigma_{xx} + (1-2\alpha_2)\Sigma_{zz}$$

(Eq. (4) of Part I), Eq. (A.1) may be solved with respect to Σ_{xx} and Σ_{zz} to yield

$$\begin{cases} \frac{\Sigma_{xx}}{\sigma_0} = -\epsilon(1-2\alpha_2)\mathscr{A}(\lambda) + [1 + (1-2\alpha_2)\eta]\mathscr{B}(\lambda), \\ \frac{\Sigma_{zz}}{\sigma_0} = 2\epsilon\alpha_2\mathscr{A}(\lambda) + (1-2\alpha_2\eta)\mathscr{B}(\lambda), \end{cases} \tag{A.4}$$

which is just another form of the parametrization of the criterion.

The parameter λ may be related to the components of the strain rate. Indeed, since the flow rule associated via normality to the GLD criterion reads

$$\begin{cases} D_{xx} = H\left[\frac{C}{\sigma_0^2}(2\eta\alpha_2 - 1)(\Sigma_{zz} - \Sigma_{xx} + \eta\Sigma_h) + 2\alpha_2 q(g+1)(g+f)\frac{\kappa}{\sigma_0}\sinh\left(\kappa\frac{\Sigma_h}{\sigma_0}\right)\right], \\ D_{zz} = 2H\left[\frac{C}{\sigma_0^2}(1 + \eta(1-2\alpha_2))(\Sigma_{zz} - \Sigma_{xx} + \eta\Sigma_h) + (1-2\alpha_2)q(g+1)(g+f)\frac{\kappa}{\sigma_0}\sinh\left(\kappa\frac{\Sigma_h}{\sigma_0}\right)\right], \end{cases}$$

where H denotes the plastic multiplier (Eq. (13) of Part I), it is easy to show that

[2] Note that ϵ denotes a sign, not a strain!

$$(1-2\alpha_2)D_{xx}-\alpha_2 D_{zz}=-H\frac{C}{\sigma_0^2}(\Sigma_{zz}-\Sigma_{xx}+\eta\Sigma_h), \tag{A.5a}$$

$$\operatorname{tr}\mathbf{D}+2\eta[(1-2\alpha_2)D_{xx}-\alpha_2 D_{zz}]=2Hq(g+1)(g+f)\frac{\kappa}{\sigma_0}\sinh\left(\kappa\frac{\Sigma_h}{\sigma_0}\right). \tag{A.5b}$$

Taking the ratio of these equations in order to eliminate the plastic multiplier and using Eqs. (A.1) and (A.3), one gets

$$\frac{\operatorname{tr}\mathbf{D}}{2[(1-2\alpha_2)D_{xx}-\alpha_2 D_{zz}]}+\eta=-\epsilon\frac{\kappa}{\sqrt{C}}\lambda. \tag{A.6}$$

This provides the desired relation.

Finally, note that by Eqs. (A.2) and (A.5a),

$$\epsilon=-\operatorname{sgn}[(1-2\alpha_2)D_{xx}-\alpha_2 D_{zz}]. \tag{A.7}$$

References

Benzerga, A.A., 2000. Rupture ductile des tôles anisotropes. Thèse de Doctorat, Ecole Nationale Supérieure des Mines de Paris. Paris, France.

Gologanu, M., 1997. Etude de quelques problèmes de rupture ductile des métaux. Thèse de Doctorat, Université Pierre et Marie Curie. Paris, France.

Gologanu, M., Leblond, J.-B., Perrin, G., Devaux, J., 1997. Recent extensions of Gurson's model for porous ductile metals. In: Suquet, P. (Ed.), Continuum Micromechanics. CISM Courses and Lectures no. 377. Springer, New York, pp. 61–130.

Gurson, A.L., 1977. Continuum theory of ductile rupture by void nucleation and growth: Part I – Yield criteria and flow rules for porous ductile media. ASME J. Engng. Mater. Technol. 99, 2–15.

Koplik, J., Needleman, A., 1988. Void growth and coalescence in porous plastic solids. Int. J. Solids Struct. 24, 835–853.

Leblond, J.-B., Perrin, G., 1996. Introduction à la mécanique de la rupture ductile des métaux. Cours de l'Ecole Polytechnique, Palaiseau, France.

Pardoen, T., Hutchinson, J.W., 2000. An extended model for void growth and coalescence. J. Mech. Phys. Solids 48, 2467–2512.

Perrin, G., 1992. Contribution à l'étude théorique et numérique de la rupture ductile des métaux. Thèse de Doctorat, Ecole Polytechnique, Palaiseau, France.

Rudnicki, J.W., Rice, J.R., 1975. Conditions for the localization of deformation in pressure-sensitive dilatant materials. J. Mech. Phys. Solids 23, 371–394.

Thomason, P.F., 1985. Three-dimensional models for the plastic limit-loads at incipient failure of the intervoid matrix in ductile porous solids. Acta Metall. 33, 1079–1085.

Tvergaard, V., 1981. Influence of voids on shear band instabilities under plane strain conditions. Int. J. Fract. 17, 389–407.